HOSTED BY

ELSEVIER

Available online at www.sciencedirect.com

ScienceDirect

Soils and Foundations 60 (2020) 1036–1049

SOILS AND FOUNDATIONS

www.elsevier.com/locate/sandf

Technical Note

Design and performance of the Quxue asphalt-core rockfill dam ☆

Shan Feng [a], Weibiao Wang [a,*], Weihua Hu [b], Yiguo Deng [c], Jian Yang [c], Shaoqiao Wu [b], Chenliang Zhang [c], Kaare Höeg [d]

[a] *Xi'an University of Technology, 5 Jinhua South Road, 710048 Xi'an, China*
[b] *Datang Xiangdian Derong Power Development Co., Ltd., 627950 Derong County, Sichuan Province, China*
[c] *POWERCHINA Beijing Engineering Corporation Limited, 1 West Street, Dingfuzhuang, Chaoyang District, 100024 Beijing, China*
[d] *Norwegian Geotechnical Institute, P.O. Box 3930, Ullevaal Stadion, NO-0806 Oslo, Norway*

Received 2 July 2019; received in revised form 31 March 2020; accepted 21 June 2020
Available online 7 August 2020

Abstract

The design and performance of the 174-m high Quxue asphalt-core rockfill dam in Sichuan Province, China, are presented. An extensive field monitoring program was implemented. During construction, the asphalt core settled more than the adjacent transition zones, but no more than 20 mm due to strong interlocking with the coarser gravel particles in the transition zones. The lateral displacements of the core were recorded during the impoundment. The measured shear displacements were less than 10 mm between the core and the plinth along the steep abutments (about 70°), and the interface remained watertight. The dam was constructed in about one year, and the reservoir impoundment up to about 100 m height was done in two months. The performance monitoring documents that the asphalt core type of dam is suitable for high embankment dams even in narrow valleys with steep abutments. The core exhibits flexible and ductile behavior without cracking, and internal core erosion is not an issue of concern.

Keywords: High embankment dam; Narrow valley; Asphalt core; Field instrumentation and monitoring

1. Introduction

Asphalt-core embankment dams (ACEDs) are being built worldwide, many of them constructed on sites with challenging topographical, geological and seismic conditions. Hydropower and Dams (2019) provides a listing of ACEDs that have been built and are under construction and design in several countries. Among the ACEDs built is the 128-m high Storglomvatn ACRD by the Arctic Circle in Norway, completed in 1997 (Höeg et al., 2007). The 125-m high Yele ACRD in China is located in a very seismic region with a design peak horizontal ground acceleration of 0.45 g. The dam is founded on a geologically complex foundation, partly resting on a deep and pervious alluvial overburden and partly on bedrock. It was completed in 2005 (Wang and Höeg, 2010; Wang et al., 2010).

Comprehensive investigations have been done to study the behavior of the asphalt core under various conditions. Zhang et al. (2013) investigated the watertightness of asphalt concrete in bending and tension to determine the magnitude of strain before cracking occurred. Crack self-healing, stress relaxation and crack-resistance at low temperature were studied. Wang and Höeg (2009) investigated the effects of different compaction methods in the laboratory on the stress-strain behavior of asphalt concrete. They found that the behavior of asphalt concrete prepared by compaction methods in the laboratory was quite different

Peer review under responsibility of The Japanese Geotechnical Society.
* Corresponding author.
E-mail addresses: fengshan@xaut.edu.cn (S. Feng), weibiaowang@xaut.edu.cn (W. Wang), 526573783@qq.com (W. Hu), dengyg@bhidi.com (Y. Deng), yangj@bhidi.com (J. Yang), 81766867@qq.com (S. Wu), zhangchl@bhidi.com (C. Zhang), kaare.hoeg@ngi.no (K. Höeg).

https://doi.org/10.1016/j.sandf.2020.06.008

from that of the roller compacted asphalt in the field. Zhang et al. (2015) investigated the conditions of hydraulic fracturing for asphalt core in dams and concluded that "hydraulic fracturing" could not occur under normal conditions. Wang and Höeg (2016) proposed a simplified material model for analysis of asphalt core in embankment dams based on long-term creep test results and slow unloading-reloading cycles of asphalt specimens prepared in the laboratory and in the field.

Feizi-Khankandi et al. (2008) presented the test results of asphalt concrete under cyclic loading at 5 °C and 18 °C and Wang and Höeg (2011) presented corresponding results at 3.5, 9, and 20 °C. Akhtarpour and Khodaii (2013) presented cyclic test results of asphalt concrete with different bitumen contents and cyclic frequencies at 22 °C. Feizi-Khankandi et al. (2009) also carried out shaking table model tests, and the test results showed large settlements for the top part of the transition zones adjacent to the core. Baziar et al. (2009) conducted dynamic centrifuge model tests on asphalt core dams combined with numerical analyses. The numerical results showed that the 52-m high Meyjaran Dam subjected to the maximum design level earthquake with peak ground acceleration = 0.5g, induced shear strains less than 1.0% within the core.

In order to make the connection between the asphalt core and concrete plinth watertight in dams subjected to earthquake shaking, copper waterstops are recommended, and SBS asphalt mastic should be used between the core and plinth (Wang et al., 2017a). Wang et al. (2018) also investigated the interface behavior between the asphalt core and the adjacent gravel transition zones and found that the asphalt core was interlocked with the coarse gravel particles even when the interface zone was sheared by large shear deformations. Wang et al. (2019) carried out shear tests on asphalt specimens at different temperatures and shear strain rates to investigate the stress-strain-strength behavior of asphalt concrete. They established the domains of shear modulus and shear strength values of asphalt concrete by examining and applying the time-temperature superposition principle.

In recent years, several high asphalt core embankment dams (ACEDs) were completed or are under construction. The 174-m high Quxue Dam in China and the 153-m high Zarema Dam in Ethiopia were completed in 2017, and the 167-m high Moglicë Dam in Albania was completed in February 2019. The 129 m high Dashimen asphalt core sand-gravel dam (ACGD) located in a narrow valley and in a very seismic region with a design peak horizontal ground acceleration of 0.52 g in China was completed in November 2019. The 129 m high Bamudun ACGD also located in a very narrow valley in China, are now under construction. The KSM-Water Storage Dam with a height of about 150 m in Canada and Frieda River Dam with a height of 185 m in Papua New Guinea, are currently under preliminary design. Recently, Höeg and Wang (2017) presented design experience and guidelines for high ACEDs, and The International Commission on Large Dams (ICOLD) has issued a third version of the bulletin on ACEDs (ICOLD, 2018).

Wang et al. (2017) reported the design and construction of the 174-m high Quxue ACRD. The dam is located in a narrow valley with a steep left abutment of 1 V: 0.33H in a region with significant seismicity. As the Quxue Dam is extensively instrumented and monitored, this paper presents the field performance observations that may be used in the future design and construction of even higher ACEDs. Emphasis is placed on the performance of the asphalt core and its interaction with the adjacent transition zones.

2. Quxue dam site conditions

The Quxue hydro project with an installed capacity of 246 MW is located on the Shuoqu River which is the largest tributary of the Dingqu River, the first tributary of the Jinsha River. The dam is located in the Derong County, Ganzi Tibetan Autonomous Prefecture, Sichuan Province. However, the main part of the reservoir area is in the Shangri-la County, Diqing Tibetan Autonomous Prefecture, Yunnan Province. The dam site is about 126 km from Shangri-la County Town.

The dam site is in mountainous terrain, and the cross-section of the narrow valley appears as an asymmetrical "V" shape. The average slope of the left bank is about 70°, and the slope of the right bank is also very steep towards the top. The width of the valley is about 200 m at the normal water storage level (NWL el.2330 m.asl.), and the ratio of valley width to valley depth at that level is about 1.3. The exposed rock at the dam site is marbleized, fine-grained limestone, and the saturated compressive strength of the moderately and lightly weathered rocks is between 40 and 60 MPa. Most of the exposed rocks are weakly weathered but with strong surface weathering of the rock in the right bank. The depth of the weathered rock is between 11 and 35 m in the river bed, 12–63 m in the left bank and 7–65 m in the right bank, respectively. Unloading fissures are developed due to the deep-cut, high and steep banks. The horizontal thicknesses of the unloading zones in the left bank are about 15 m at el.2222.0 m.asl. and 38–63 m at el.2280.0 m.asl. In the right bank the unloading zones are 25–50 m at el.2220.0 m.asl., about 30 m at el.2280. m.asl., and 15–21 m at el.2330.0 m.asl.

There are no primary regional faults crossing the dam foundation, but there is one main secondary fault joint in the left abutment (shown as No.7 in Fig. 3) with a fractured zone width of 30–100 cm. There are several small secondary fault joints in the right abutment with steep dips and fractured zone widths of 2–40 cm. Furthermore, in the right bank there are two groups of various size karst caves. The first group of karst caves (shown as No.8 in Fig. 3) are relatively large with a trend intersect with the river at a small angle. The caves are interconnected and filled with grayish-white calcareous and purple-red mud. The second group of three karst caves are exposed on the

surface and located downstream about 260 m from the dam axis with a trend nearly vertical intersect with the river. The main leakages in the dam site region are from cracks/solution cracks and channels, and some leakages from structural planes in the rock.

The depth to bedrock under the alluvial river overburden is about 30 m at the dam site.

For the topographical shape and the geological conditions, an RCC arch dam, a CFRD and an ACRD were examined and compared. The asphalt-core rockfill dam option was selected as presented by Wang et al. (2017).

3. Asphalt core dam design

Fig. 1 shows the ACRD cross-section that was selected. The asphalt core in that cross-section is 132 m high from el.2201.0 m.asl. to el.2333.0 m.asl., and the total dam height is 174 m from el.2160.0 m.asl. to el.2334.2 el.asl.. The crest length for the dam is 220 m. Due to the seismicity of the region, the dam is designed with a gentle upstream slope of 1 V:1.9H, an average downstream slope of 1 V:1.84H, and a wide crest of 15 m. The downstream slopes between the 10 m wide road berms are steep, 1 V:1.3H. As an earthquake-resistant measure, bi-directional polypropylene geo-grids with a vertical distance of 2.4 m between the geo-grids were placed horizontally to reinforce the top 30 m of the dam (from el.2305.0 m.asl. to the dam crest at el.2334.2 m.asl.).

The vertical asphalt core wall, located 2.0 m upstream of the dam centerline, is designed to be 1.5 m wide at the bottom and decreasing gradually to 0.6 m at the top (el.2333.0 m.asl). Comprehensive test investigations were conducted on the materials and on mixes for the asphalt core, and the bitumen type B70 was selected. The aggregates were crushed limestone and the added filler consisited of limestone powder. The total filler content was 13% and the bitumen content 6.8% by the mineral weight. The base of the core is flared out against the foundation concrete plinth (concrete monolith in Fig. 1) to a width of 3.0 m at the core-plinth interface. Similarly, the core is flared out against the plinth at the abutments to double the core width at the interface. Fig. 2 shows the top shape of the foundation plinth and the plinth along the left abutment. To ensure that the connection of the asphalt core with the plinth is watertight, one row of copper waterstop was installed along the core axis. The surface of the plinth under the core was made concave with a maximum depth of 25 cm at the core centerline. The top width of the foundation plinth is 8 m, and the width of the plinth anchored in the rock along the abutments is 8 m at the bottom and is gradually reduced to 5 m at the top. In order to provide a smooth abutment profile for the asphalt core and a stable concrete plinth along the steep rock abutments, the plinth was desgined to be embedded in the rock abutments (Fig. 2). For that purpose the thickness of the plinth normal to the slope came out to be in the range of 3–5 m to obtain a satisfactory profile along the rough abutments.

The width of the upstream and downstream fine transition zones (Zone 2) adjacent to the asphalt core is 2.0 m, and the width of the upstream and downstream coarse transition zones (Zone 3) is 4.0 m at the bottom and 2.0 m at the top (see Fig. 1). In order to reduce the settlements of the rockfill in the lower central part of the dam, especially well compacted rockfill (Zone 5 in Fig. 1) was placed adjacent to the upstream and downstream coarse transition zones.

Fig. 3 shows the longitudinal section along the asphalt core axis and the layout of the grouting galleries and grout curtains in the foundation.

4. Dam construction progress and reservoir impounding

The construction of the dam base concrete monolith across the river channel started 28 January 2015 and was

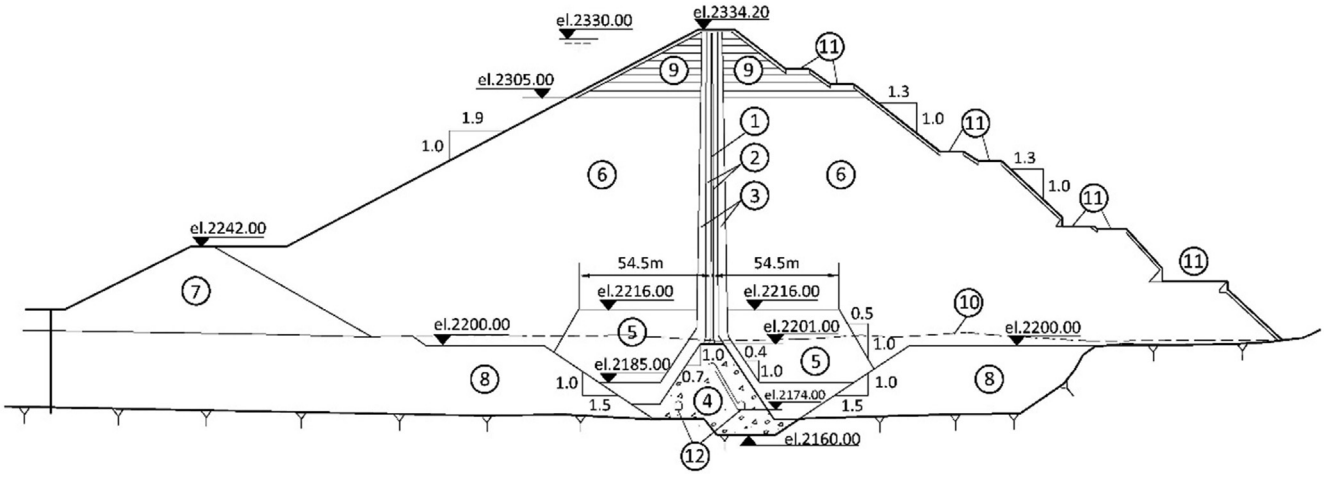

Fig. 1. Cross-section of the Quxue Dam (see location of cross-section A in Figs. 5 and 7). (1) asphalt core; (2) fine transition zone; (3) coarse transition zone; (4) concrete monolith; (5) especially well compacted rockfill; (6) rockfill; (7) upstream cofferdam; (8) alluvial overburden; (9) bi-directional polypropylene geo-grids; (10) natural ground surface; (11) 10 m wide road berm; (12) transportation and grouting galleries.

Fig. 2. View of the top of the foundation plinth and the plinth along the left abutment.

completed 31 May 2015. Embankment fill construction started 13 April 2015, and the top of the asphalt core was reached 27 February 2017 at el.2333.35 m.asl. The design elevation for the top of core was el.2333.0 m.asl., but the core was built to el.2333.35 m.asl. to compensate for the estimated settlement after construction.

The reservoir impounding started on 12 February 2017 from el. 2208 m.asl., and on 17 June 2017 the water level reached el.2320 m.asl. which is 10 m below the NWL at el. 2330 m.asl. The water level at el. 2320 m.asl. was kept for the flood season from June to October. On 30 July 2017, the Quxue hydropower station started to generate electricity. In November 2017, the water level reached el. 2327 m.asl. only 3 m below the NWL. Fig. 4 shows the progress of dam construction, impounding and operation until November 2017.

5. Dam monitoring and performance observations

An extensive field instrumentation and monitoring program is implemented on the Quxue Dam. The monitoring system consists of measuring dam body deformations, asphalt core deformations, settlement differences between the core and adjacent transition zones, strains and temperatures in the asphalt core, concrete plinth deformations, joint movements between the slabs of the plinth, forces in the steel reinforcement and in the anchor bolts for the plinth, strains in the plinth, water pressures in the abutments and foundation, seepage through the core, and dynamic response during any earthquake shaking.

Fig. 5 shows an overview of the dam with the locations of the instrumented cross-sections A, B and C. The distances of the cross-sections from the left bank are 70 m (A), 140 m (B) and 40 m (C), respectively. All the measurements inside the dam are collected at the five observation huts on the downstream dam slope and through pipes up to the dam crest.

6. Internal settlements during dam construction

The vertical settlements inside the dam are obtained by water level gages, and the horizontal displacements are obtained by extensometer measurements relative to the movements recorded at the five observation huts at the downstream slope of the dam (see numbers 11 in Fig. 5). The settlement and displacement measurements were scheduled to start during construction as soon as the instruments were installed at the predetermined levels. Unfortunately, this did not occur, and the measurements of horizontal displacements started long after instrument installation. Furthermore, the records of displacements are discontinuous and incomplete. The record of vertical settlement measurements is also incomplete with gaps in the data files. Therefore, there can be no detailed presentation of internal vertical and horizontal displacements during construction. However, there is a complete record of lateral core displacements since start of reservoir impounding.

7. Performance of asphalt core

Fig. 6 shows the arrangements of inclinometers, settlement difference meters, strain meters, thermometers and piezometers in cross-section A. The arrangements of the same types of instruments in cross-sections B and C are similar to those in cross-section A.

7.1. Displacements since start of reservoir impounding

SAA (Shape-Accel-Array) type inclinometers, installed on the downstream face of the asphalt core in cross-sections A, B and C, measured the displacements of the core in the upstream-downstream and longitudinal (left-right bank) directions since the start of reservoir impounding. The SAA inclinometers are MEMS (micro-machined) acceleration type meters with a resolution of 0.005° (per section) and an absolute error of whole section of −1.5 to 1.5 mm/32 m. They are used in a temperature range of −20 °C to 60 °C and have a waterproof capacity of 100 m water head. The casings for the inclinometers were installed on the downstream face of the core during dam construction, and the SAA sensors were put into the casings from the dam top after dam construction. Unfortunately, the casings in cross-sections B and C were clogged

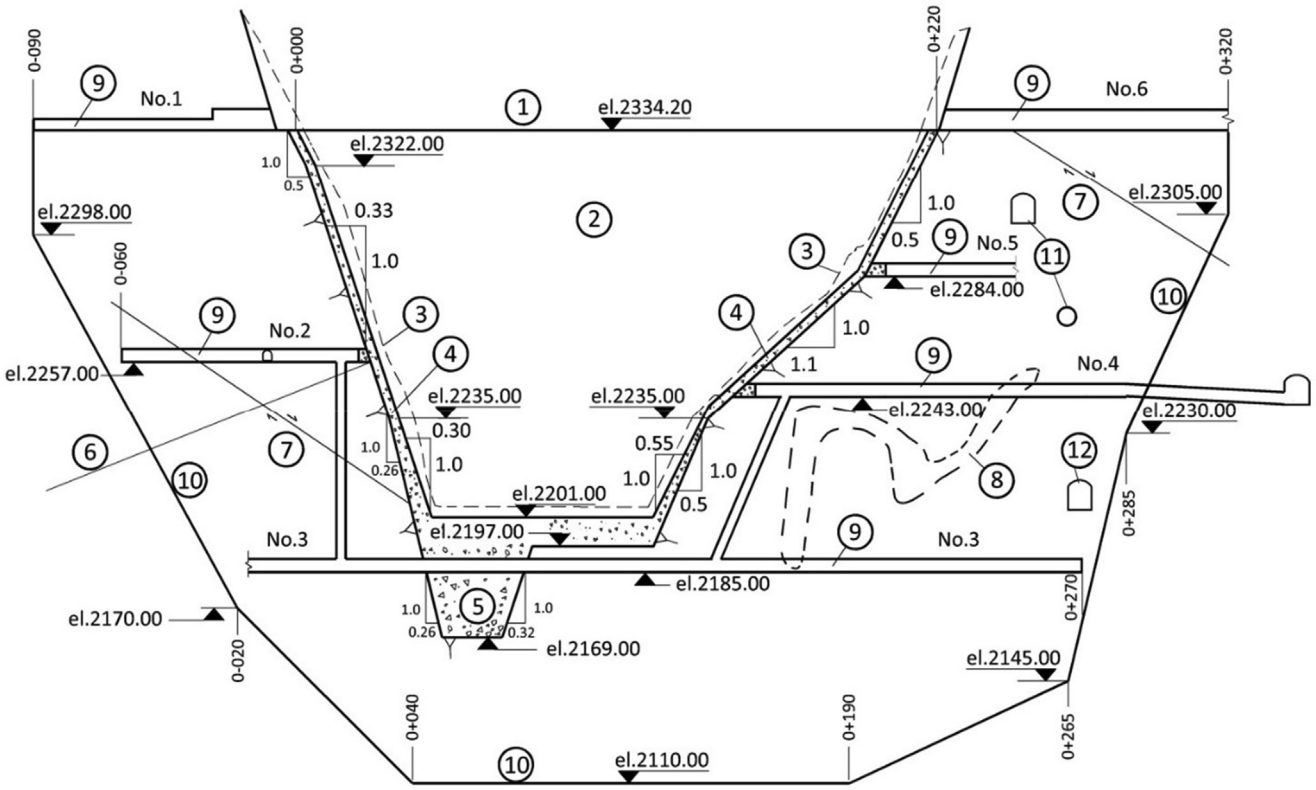

Fig. 3. Longitudinal section along the asphalt core axis showing grouting galleries in the foundation. (1) crest; (2) asphalt core; (3) ground surface; (4) concrete plinth; (5) dam base concrete monolith; (6) rock joint; (7) fault; (8) karst caves filled with cement after being washed; (9) grouting and transportation gallery; (10) bottom level of grout curtain; (11) spillway tunnel; (12) diversion tunnel.

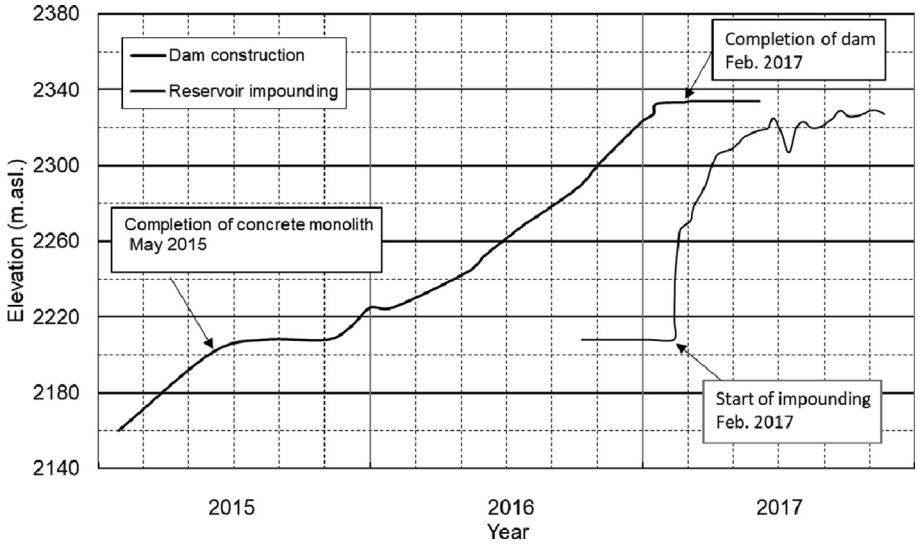

Fig. 4. Progress of dam construction and reservoir impounding.

at el.2269.0 m.asl. and el.2257.0 m.asl., respectively, by accidentally falling stones, so the SAA sensors were unable to reach the bottom design elevations through the casings. Fig. 7 shows the measured results.

For cross-section A in Fig. 7 (a), when the reservoir water level reached el.2320 m.asl. in June 2017, the top of the core had moved in the upstream direction about 20 mm. In November 2017 with water level at el. 2327 m. asl., the top of the core had moved in the downstream direction by about 15 mm caused by downstream creep and the water level increase of 7 m. Most of the core moved downstream with a maximum of about 90 mm at el.2230 m.asl. It should be noted that the displacements of the core presented in cross-sections B and C are the

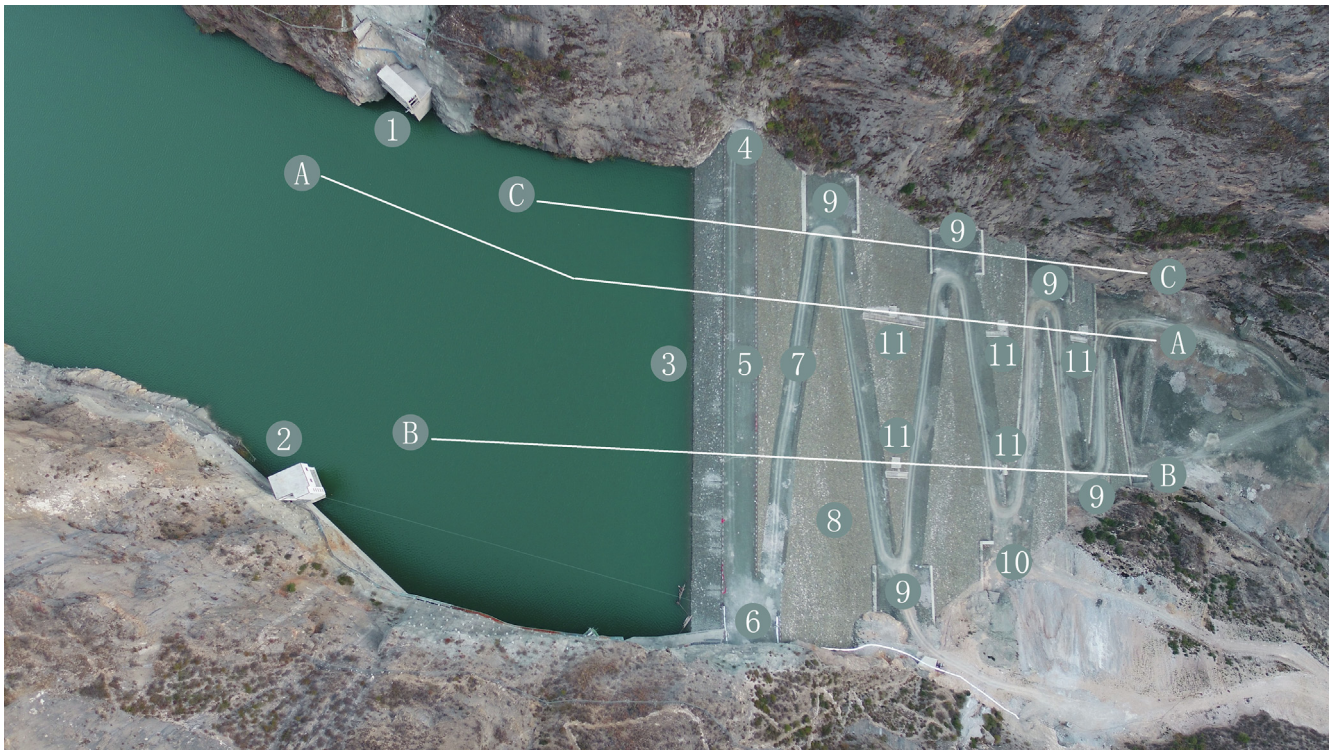

Fig. 5. Overview of the Quxue Dam and locations of instrumented cross-sections A, B and C. (1) inlet of hydropower tunnel; (2) inlet of spillway tunnel; (3) water level at el.2327 m.asl., which is 3 m below the NWL at el.2330 m.asl.; (4) exit and entrance of transportation tunnel at left dam crest; (5) 15 m-wide dam crest at el. 2334.2 m.asl.; (6) exit and entrance of transportation tunnel at right dam crest; (7) 10 m-wide road berms; (8) downstream slope 1 V:1.3H between road berms (average slope 1 V:1.84H); (9) platforms for vehicles' "U" turn; (10) exit and entrance of transportation tunnel and platform for vehicles' "U" turn; (11) observation huts.

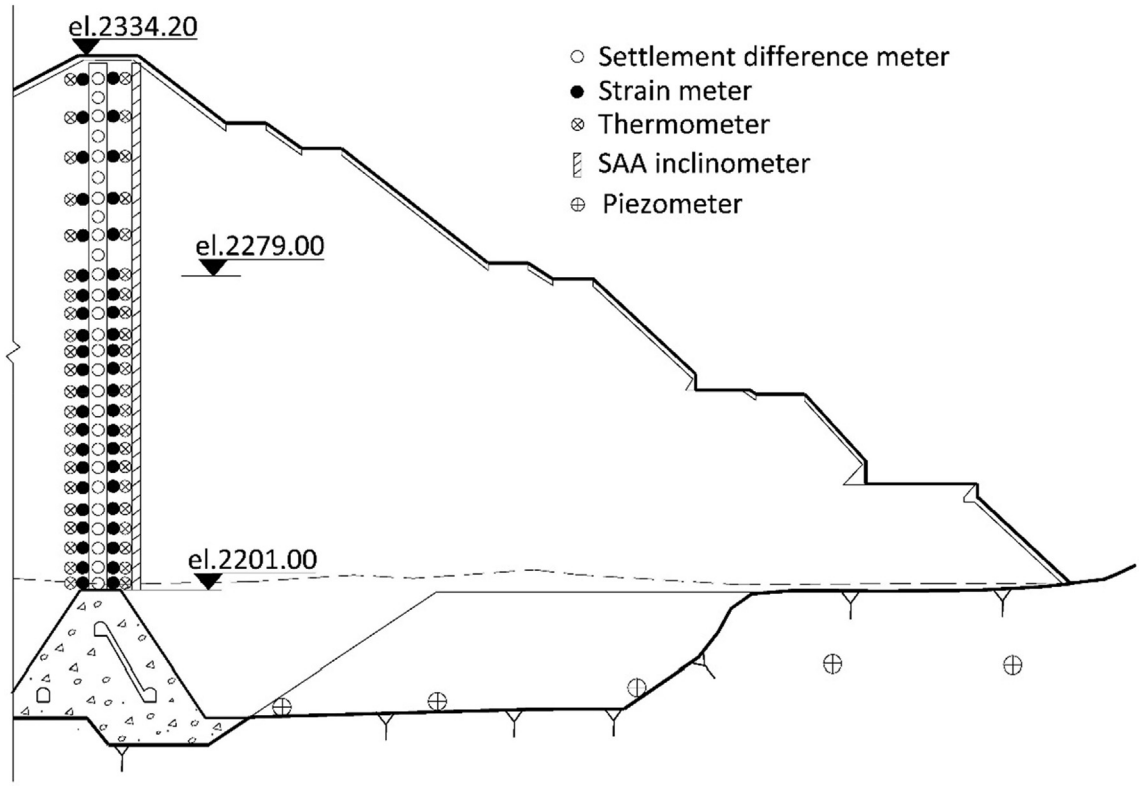

Fig. 6. Arrangement of inclinometers, settlement difference meters, strain meters, thermometers and piezometers in cross-section A.

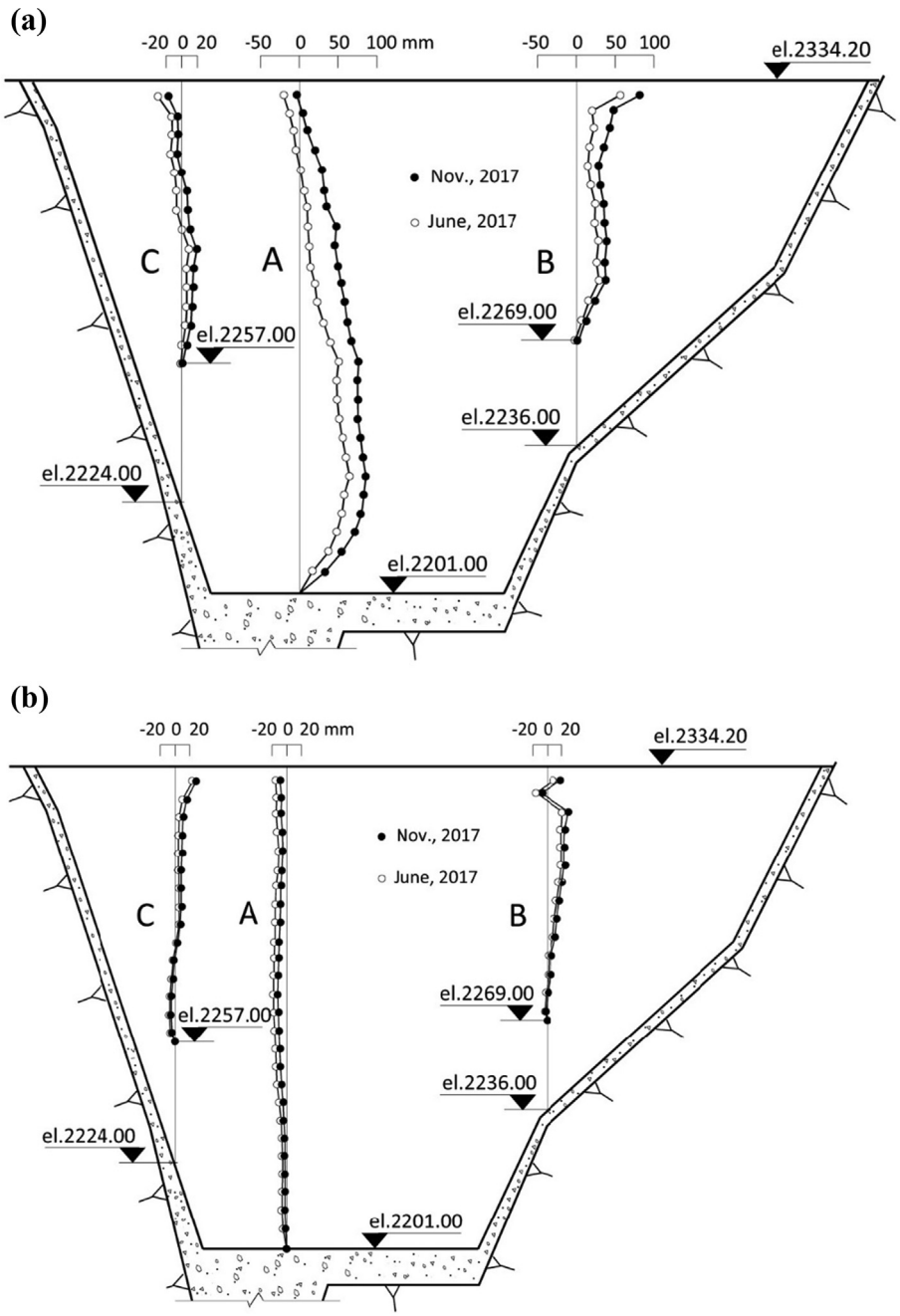

Fig. 7. Incremental displacements of the asphalt core since start of reservoir impounding. (a) Measured core displacements in the upstream–downstream direction (positive towards downstream). (b) Measured core displacements in the left–right direction (positive towards right abutment).

relative displacements to the elevations where the casings were clogged which are not the levels of casing fixity. For cross-section B, the core moved in the downstream direction with a maximum of about 80 mm at the top of the core in November 2017. The top of the core in cross-section C first moved upstream about 25 mm (June 2017) and then moved downstream a small amount, and was 20 mm in the upstream direction by November 2017. Fig. 8 shows in more detail the development of lateral core displacements since start of reservoir impounding. As expected, the upstream shoulder experienced settlements due to the wetting effect during impounding and that caused the top part of the core to first move in the upstream direction before it later moved downstream.

The reservoir impounding began on 12 February 2017 from el.2208 m.asl. and reached el.2280 m.asl. on 15 March. The water level increased as much as 72 m in the 31 days. This caused the core to move in the downstream direction about 20 mm at el.2230 m.asl. However, above the water level at el.2280 m.asl. the core had moved in the upstream direction by about 8 mm at the top of the core. The asphalt core seats on top of the concrete

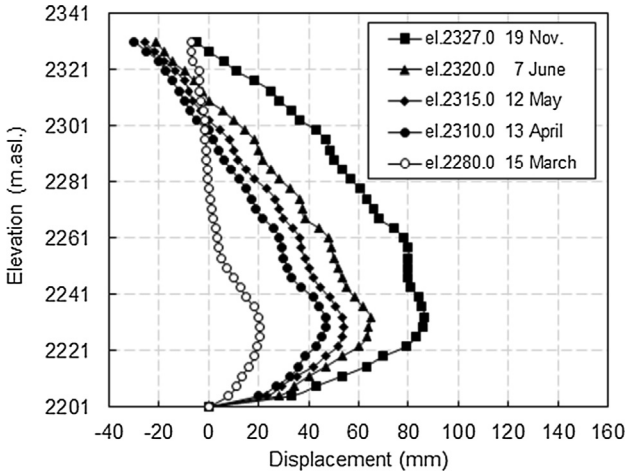

Fig. 8. Measured core displacement in the upstream–downstream direction during reservoir impounding at different reservoir water levels in cross-section A (positive towards downstream).

monolith, and there is an about 35 m deep compacted rockfill and alluvial overburden behind the monolith (see Fig. 1, Zones 5 and 8). Settlements in the deep rockfill and alluvial overburden contributed to the large lateral displacements towards the bottom of the core (Fig. 8). When the water level reached el.2310 m.asl. on 13 April, the core had moved downstream with a maximum displacement of about 45 mm at el.2230 m.asl. and upstream with a maximum displacement of about 30 mm at the top of the core. When the water level reached el.2327 m.asl. on 19 November, the lateral displacement curve shows a maximum downstream displacement of about 90 mm at el.2230 m.asl. and an upstream displacement of 5 mm at the top of the core.

Fig. 7(b) shows very small displacements of the core in cross-section A in the left-right direction since start of reservoir impounding.

7.2. Settlement differences between the core and the fine transition zone (Zone 2)

Special gages installed at the upstream and downstream interfaces between the core and the fine transition zones measured the settlement differences between the core and the fine transition zones at different elevations in cross-sections A, B and C. The special gages are vibrating wire settlement difference meters with a maximum survey range of up to 150 mm. The meters installed below el.2232.0 m.asl. on the upstream face of the core have a water bearing pressure capacity of 2.0 MPa while the meters installed between el.2232.0 m.asl. and el.2282.0 m.asl. on the upstream face of the core have a water bearing pressure capacity of 1.0 MPa. The other meters have a water bearing pressure capacity of 0.5 MPa. One end of the meter is a steel bar that is fixed in the asphalt core while other end is a steel plate that is placed in the fine transition zone. The sensor of the meter between the two ends measures the vertical settlement difference between the core and the fine transition zone. The measurement points were arranged with an individual height difference of 5 m below el.2279 m.asl. and 10 m above that elevation. Fig. 9 shows the measured results at the end of dam construction in February 2017 and also in November 2017 after the reservoir impounding and some creep deformations had taken place.

The data in Fig. 9 show that there are significant variations in the locally measured settlement differences over the core height. When the gages were installed during construction, the asphalt core was still hot and soft. The asphalt core is in contact with Zone 2 material with particle size 0–60 mm, and the particle size may have caused significant variations in the locally measured settlement differences. In general, the asphalt core settled more than the transition zone, and the settlement differences took place mostly during the dam construction period. There is a relatively insignificant increase in the settlement differences due to reservoir impounding and creep. There is only one exception to this finding, and that is the measured increase in settlement difference at the downstream side of the core in cross-section A at el.2236.0 m.asl. (Fig. 9b). However, this data point seems to be an outlier. The measured settlement differences are in general agreement with the findings for the Maopingxi Dam and the Yele Dam in China (Wang et al., 2010).

Fig. 9 shows that most of the measured local settlement differences are less than 20 mm, and the magnitudes of the settlement differences do not seem to be related to the height above the base of the core. Only a few of the settlement differences were larger than 20 mm, but all less than 30 mm at the downstream side of the core in cross-sections B and C (Fig. 9b). In cross-section A below el.2229.0 m.asl. the settlement difference increased towards the base of the core. The maximum settlement differences at el.2204.0 m.asl. at end of dam construction were 30 mm on the upstream side of the core (Fig. 9a) and 26 mm on the downstream side of the core (Fig. 9b). The width of the core at el.2204.0 m.asl. is 1.5 m, and it gradually increases to 3.0 m towards the top of the monolith at el.2201.0 m.asl. The flared region of the asphalt core maintains high temperatures for a longer time, and this may result in increased core settlement in the flared part.

The asphalt core and the adjacent fine transition zones on either side of the core are placed in the same construction operation with a compacted layer thickness of 20–25 cm. The interface on the upstream and downstream sides of the core will in field practice show a zigzag pattern due to the method of construction (Höeg, 1993). The asphalt core-gravel interface is strongly interlocked, but with time the core tends to settle more than the transition zones due to the core's creep behavior. Field measurements from other ACRDs show maximum settlement differences between the asphalt core and transition zones to be in the range of 20–50 mm (Wang et al., 2010). Laboratory model test results confirm that the asphalt core face does not detach from the fine gravel transition zone even for large

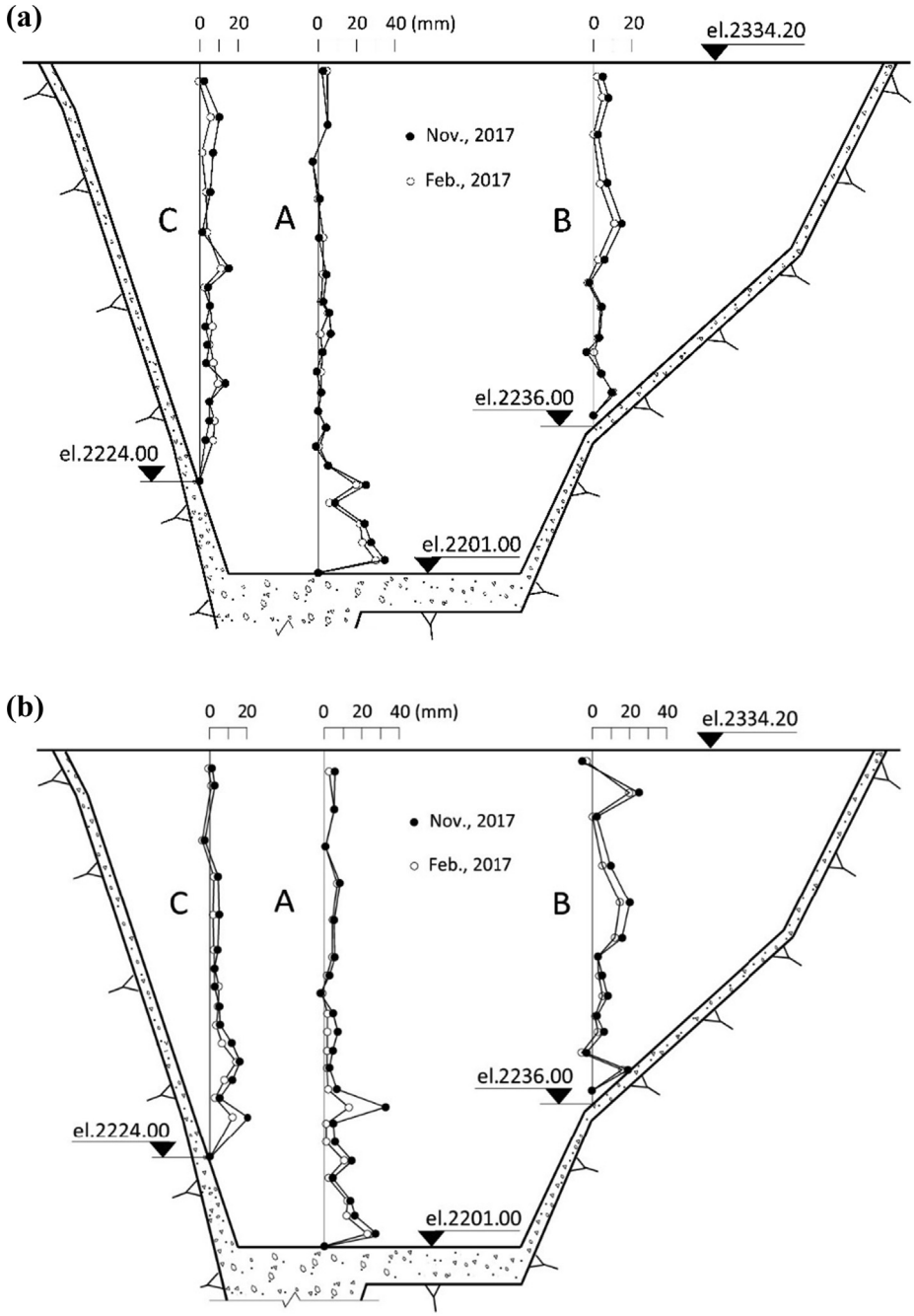

Fig. 9. Measured settlement differences between the core and the adjacent fine transition zones at the end of dam construction and after the reservoir impounding. Positive value means that the core settled more than the adjacent transition zone. (a) Upstream side of core. (b) Downstream side of core.

shear displacements (Wang et al., 2018). The laboratory test results also show that the hydro-mechanical properties of the thin shear zones on either side of the core do not deteriorate due to the differential settlements. However, due to the fact that the core tends to "hang" on the adjacent fine transition zones (arching), the vertical stresses in the core are lower than the vertical overburden stress. This arching effect has been measured in several ACEDs (Wang et al., 2010).

7.3. Measured strains in the core face

Two-orthogonal joint meters with a clean distance of 315 mm were installed at the upstream and downstream asphalt core faces to measure the local core strains in the vertical and longitudinal directions at different elevations in cross-sections A (Fig. 6), B and C. The measuring points were arranged to be the same as for the differential settlement measurements between the core and transition zones.

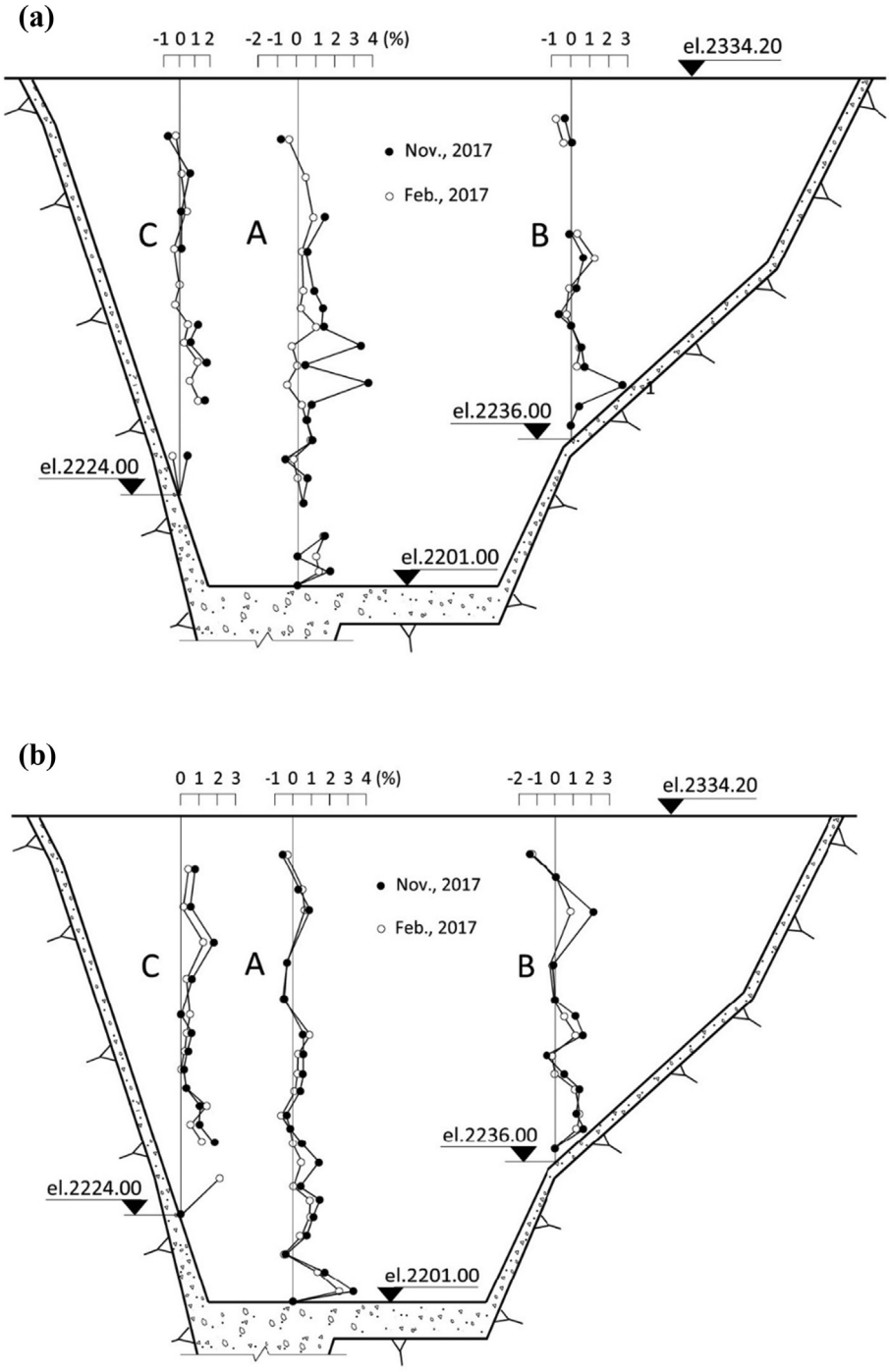

Fig. 10. Measured vertical strains in the core faces at end-of-construction and after impounding. Positive value means that the core face is in compression. (a) Upstream face, (b) Downstream face.

Fig. 10 shows the measured local vertical strains in the core faces at the end of dam construction in February 2017 and in November 2017 after reservoir impounding.

Many of the joint meters were damaged or gave erroneous data. The joint meters anchored on the faces of the core were affected by the initial softness of the core, and the measurements were disturbed by the coarse gravel particles. However, the general conclusions from the large number of measured values are that the vertical and longitudinal strains in the upstream and downstream faces of the core were all compressive and in magnitude less than about 4.0% and 3.0%, respectively. The reservoir impounding had insignificant effects on the magnitudes of the strains in the core faces.

7.4. Temperature in the asphalt core

Forty-four (44) thermometers were installed in the asphalt core in cross-sections A (Fig. 6) and B with an individual height difference of 5 m to cover the whole height of

the core. Twenty-four (24) thermometers were installed in three consecutive layers during construction and in four different locations in the lower part of the asphalt core. The thermometers started to record the temperature in the core immediately after they were installed at the different elevations. The measured results are shown in Table 1.

The temperature of the asphalt core was in the range of 145–165 °C during placing and compaction and dropped to a range of 60–100 °C in a few days. The temperature reduction in the asphalt during the first days after placement is strongly dependent on the weather conditions and how long the asphalt core is exposed before the next layer is placed. Once the asphalt is covered by the next asphalt layer, the temperature in the previous layer reduces at a very slow rate.

For the Quxue Dam asphalt core, Table 1 shows that the average temperature was about 37 °C after one month and about 21 °C half a year after the asphalt layer had been placed. The temperatures in three consecutive asphalt layers followed almost the same temperature reduction curve. After reservoir impounding, the temperature in the asphalt core dropped to a range of 13–18 °C. In November 2017, the average temperature over the height of the asphalt core was 15.3 °C.

All the thermometers showed smooth temperature reduction curves with time, and that in itself indicates that the core has no significant fissures or voids to allow local seepage/leakage through the core and thereby affect the local temperature. The data in Table 1 showing temperature reduction with time may be used in future numerical stress-strain analysis of core behavior and the sharing of loads (arching) between the core and the adjacent gravel transition zones.

8. Performance of concrete plinth under the core

The concrete plinth along the abutments was placed on a clean and fresh surface of rock and was built in slabs with slab lengths of 7–10 m along the core centerline (Fig. 2). The construction joints between the slabs were sealed with rubber and copper water stops.

The displacements of the plinth, the joints between the slabs, and the shear displacements of the core along the plinth slope were monitored. The one-way joint meters are vibrating wire displacement meters with a maximum survey range of up to 25 mm. The meters installed below el.2282.0 m.asl. have a water bearing pressure capacity of 1.5 MPa while the other meters have a water bearing pressure capacity of 0.5 MPa. The meter measures the joint opening or closing between adjacent two slabs. To measure the shear displacement between the concrete plinth surface and the base of the asphalt core one end of the meter is installed in the plinth surface while the other end is placed in the asphalt core.

Fig. 11 shows that the interface compressive displacements (D) between the plinth and the rock foundation and between the core and plinth along the steep left bank were less than about 15 mm. The reservoir impounding had insignificant effects on the compressive displacements. At about half height of the plinth on the left abutment the interface tensile displacements were smaller than 2 mm at end of the dam construction. The small interface tensile displacements were caused by the grouting uplift pressures, and the opened "gap" was simultaneously filled by the grout. After reservoir impounding the small interface tensile displacements became zero or compressive. However, at about half height along the right abutment the interface tensile displacements between the plinth and rock foundation had values (D) up to 20 mm. The rock foundation in this area is relatively weak and the plinth was probably uplifted by the grouting pressures although the plinth was anchored in the rock (Fig. 12). Some interface tensile displacements caused by the grouting were simultaneously filled by the grouting. The additional interface tensile displacements of 5–10 mm were probably caused by uplift pressures resulting from the reservoir impounding.

Fig. 11 also shows that the joints between the slabs along the plinth closed or opened less than 3 mm (J). The small joint opening displacements have no effects on the joint water tightness as the joints were provided with rubber and copper water stops.

The measured shear displacements at the interface (SD) between the core base and plinth along the left and right abutments were less than 10 mm. Most of the shear displacements took place during dam construction. Along the interface, the middle and lower part of the core sheared downwards while it sheared upwards towards the top. The small shear displacements have no effects on the watertightness of the connection between the core and the plinth. This is also documented by laboratory tests on the connection between core and plinth when using sandy asphalt mastic at the interface (Wang et al., 2010, 2017a, 2017b).

9. Measured water pressures and seepage

Twenty-five (25) piezometers were installed in the dam foundation and fourteen inside the dam. Fig. 13 shows the piezometers at the top of the concrete plinth and upstream and downstream of the asphalt core. The

Table 1
Temperature in asphalt core with time after placement of asphalt layer (°C).

Time (Month)	1/3	2/3	1	2	3	4	6	7	8	9
Range	40–68	30–55	27–48	24–38	18–36	16–35	15–33	15–32	12–30	12–25
Average	53.5	43.7	36.8	31.7	26.5	23.4	21.4	19.6	18.4	17.5

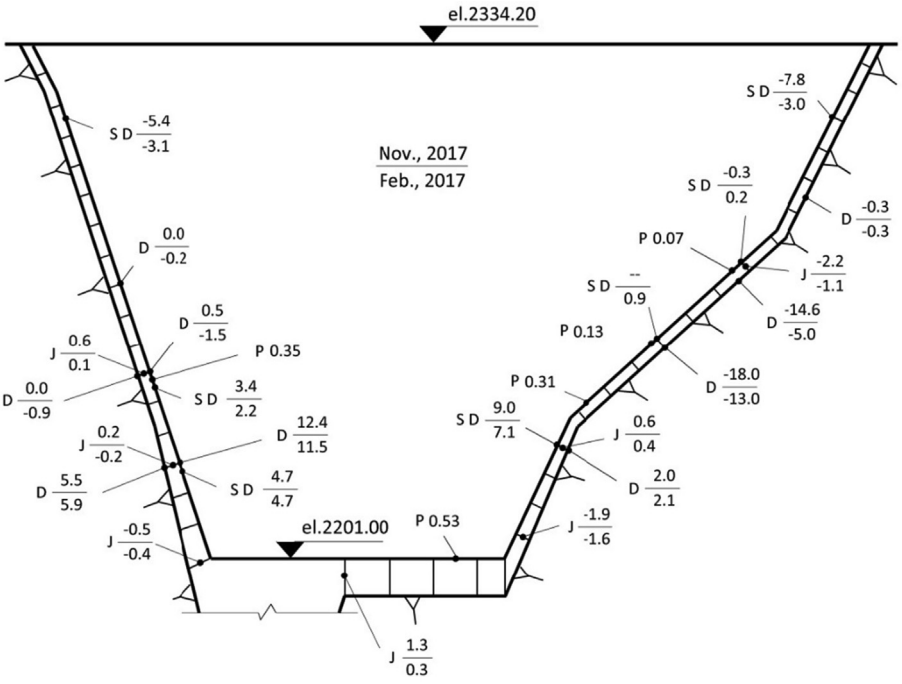

Fig. 11. Performance of the concrete plinth under the core at the end of dam construction and after reservoir impounding (unit: mm). The symbols shown in the figure are: D = displacement; J = joint opening or closing; SD = shear displacement of the core along the plinth slope. Positive value means compressive displacement, or joint closing, or core moving downwards along plinth slope.

Fig. 12. View of the weak rock foundation along the right abutment at about half height.

piezometers on the concrete plinth were arranged along and parallel to the core center line. The piezometers located in the foundation in front of the grout curtain showed good correlation between the measured water pressures and the reservoir level during the impounding. The piezometers located under the plinth on the left bank showed pressure head increases of 0–20 m as a result of reservoir impounding while the piezometers located under the plinth on the right bank showed water pressures not significantly affected by the reservoir impounding. The piezometers located in the foundation in the left and right abutments and in cross-sections B and C behind the core wall, showed that the water pressures were not significantly affected by the impounding. The piezometers located in the foundation under the downstream shoulder along cross-section A (Fig. 6) showed a pressure head increase of about 6 m as a result of the impounding.

Twenty-seven (27) piezometers were installed in the grouting and transportation galleries (see Fig. 3) and the platforms (see Fig. 5, No.9). The pressure head changes due to the impounding as measured by the piezometers are shown in Table 2.

The measured water pressures during impounding were somewhat erratic as the reservoir water gradually found its way, but the measured pressures and seepage rate values were rather stable after the impounding was completed to NWL. The stable results were used to evaluate the water-tightness of the asphalt core and the core-plinth connections. The total seepage loss is expected to reduce due to

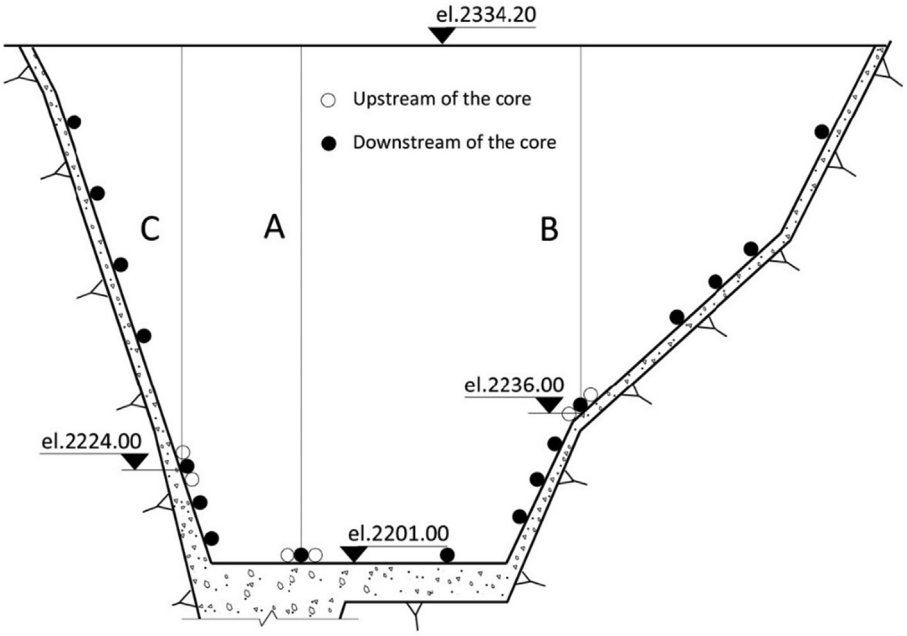

Fig. 13. Piezometers at the top of the concrete plinth and upstream and downstream of the asphalt core.

Table 2
Measured pressure head changes due to impounding.

Location	No.1 and No.5 galleries[1]	No.2,No.3,No.4 galleries[1]	Platforms[2]	Gallery at el.2174 m.asl. [3]
Water pressure change (m)	0–15	0–46	5–15	5–20

[1] The galleries are shown as No.9 in Fig. 3.
[2] The platforms are shown on the dam downstream slope as No.9 and No.10 in Fig. 5.
[3] The gallery is in the low part of the monolith and is shown as No.11 in Fig. 1.

siltation and sealing of joints in the foundation and abutments.

Four seepage measuring weirs were installed in grouting gallery No.3 and two in each of the galleries No.2, No.4, and No.5 (see Fig. 3). One weir was installed in the transportation gallery in the left bank that connects to gallery No.3 and one in the transportation gallery in the right bank that also connects to gallery No.3. One weir was installed in a branch gallery in the downstream of the right bank that connects to gallery No.3. One weir was also installed downstream cofferdam. In total, 14 weirs were installed.

The total seepage in the 10 weirs in galleries No.2, No.3, No.4 and No.5 was 11.6 L/s in November 2017. The seepages in the two weirs in the transportation galleries that connect to gallery No.3 in the left and right banks were 23.8 L/s and 6.7 L/s, respectively. Parts of the seepages (23.8 L/s and 6.7 L/s) stemmed from temporary construction activities in the galleries. The measured seepage at the weir in the branch gallery downstream of the right abutment was 40.0 L/s.

The weir in the downstream cofferdam measuring seepage through the asphalt core wall, the concrete plinth and under the plinth amounted to 17.4L/s in June 2017, 12.6 L/s in November 2017, 0.8 L/s in May 2018, respectively. It should be noted that the period from June to October is the rainy season in the region and the seepage measured during the rainy season includes some rainfall.

Based on the measured water pressures in the dam and its foundation and on the measured seepages, one may conclude that the Quxue ACRD performs as intended.

10. Concluding remarks

For the narrow valley with steep abutments at the Quxue Dam site, a rockfill dam with a central core of asphalt concrete was selected rather than an RCC arch dam option or a CFRD (Wang et al., 2017a, 2017b). The dam was built in about one year, and the reservoir level was subsequently raised by about 100 m during the subsequent 2-month period. An extensive field monitoring program was implemented for the Quxue Dam, with emphasis on the core performance and the interaction with the adjacent transition zones. The field measurements resulted in the following findings and conclusions.

- Previous experience has shown that the asphalt core generally settles more than the adjacent transition zones.

For the high Quxue Dam the maximum difference between the settlement of the core and the adjacent transition zones was about 20 mm.

- During impoundment the maximum lateral downstream displacement of the core was 90 mm 30 m above the plinth on top of the concrete monolith, while the top of the core moved 5 mm in the upstream direction.
- The asphalt core was placed and compacted with a temperature of 145–165 °C, and the temperatures dropped to a range of 60–100 °C in a few days. The average temperature was about 37 °C after one month and about 21 °C half a year after an asphalt layer was placed. After reservoir impounding, the temperature of the asphalt core dropped to a range of 13–18 °C. The measured temperatures are useful for analyzing and evaluating the asphalt core behavior during construction and operation of future ACEDs as asphalt behavior is strongly time and temperature dependent.
- The measured shear displacements between the base of the core and the plinth along the steep abutments were less than 10 mm, and the interface remained watertight. This finding should reduce concerns about the core-plinth connection behavior along a plinth even as steep as 1 V:0.33H.

Based on the field measurements, one may conclude that the asphalt core of the Quxue Dam performs well. There are no indications of any fissuring or cracking resulting in leakage through the core or at the core-plinth interface. The field observations document that the flexible and ductile asphalt core is very suitable for use in high embankment dams even when located in complex topographic and geological conditions.

Acknowledgements

The research work for the paper was partly funded by the National Science Foundation of China (No.51179155). The field monitoring data presented in the paper is primarily extracted from the field performance observation report of November 2017 provided by the monitoring unit of POWERCHINA Zhongnan Engineering Corporation Limited, and their support is gratefully acknowledged.

References

Akhtarpour, A., Khodaii, A., 2013. Experimental study of asphaltic concrete dynamic properties as an impervious core in embankment dams. Constr. Build Mater. 41, 319–334.

Baziar, M.H., Salemi, S.H., Merrifield, C.M., 2009. Dynamic centrifuge model tests on asphalt-concrete core dams 59(9):763:771. Géotechnique.

Feizi-Khankandi, S., Mirghasemi, A.A., Ghalandarzadeh, A., Höeg, K., 2008. Cyclic triaxial tests on asphalt concrete as a water barrier for embankment dams. Soils Found. 48 (3), 319–332.

Feizi-Khankandi, S., Ghalandarzadeh, A., Mirghasemi, A.A., Höeg, K., 2009. Seismic analysis of the Garmrood embankment dam with asphaltic concrete core. J. Soils Found. 49 (2), 153–166.

Höeg, K., Vastad, T., Kjaernsli, B., Ruud, A.M., 2007. Asphalt core embankment dams: resent case studies and research. Hydropower and Dams 13 (5), 112–119.

Höeg, K., Wang, W., 2017. Design and construction of high asphalt core embankment dams. International Symposium on Knowledge Based Dam Engineering, Prague, Czech Republic, July 5

Hydropower & Dams, 2019. Asphaltic concrete core dams. Listing in H&D World Atlas and Industry Guide

ICOLD, 2018. Asphalt concrete core for embankment dams. International Commission on Large Dams, Bulletin 179, Paris, France.

Wang, W., Feng, S., Zhang, Y., 2017a. Investigation of asphalt core-plinth connection in embankment dams. Case Stud. Constr. Mater. 7, 305–316.

Wang, W., Hu, K., Feng, S., Li, G., Höeg, K., 2019. Shear behavior of hydraulic asphalt concrete at different temperatures and strain rates. Constr. Build. Mater. 230 (2020), 117022.

Wang, W., Feng, S., Zhang, Y., 2018. Investigation of interface between asphalt core and gravel transition zone in embankment dams. Constr. Build. Mater. 185 (2018), 148–155.

Wang, W., Höeg, K., 2009. Method of compaction has significant effects on stress-strain behaviour of hydraulic asphalt concrete. J. Test. Eval., Am. Soc. Testing Mater. (ASTM) 37 (3), 264–274.

Wang, W., Höeg, K., 2010. Developments in the design and construction of asphalt core dams. Hydropower and Dams 17 (3), 83–91.

Wang, W., Höeg, K., Zhang, Y., 2010. Design and performance of the Yele asphalt-core rockfill dam. Can. Geotech. J. 47 (12), 1365–1381.

Wang, W., Höeg, K., 2011. Cyclic behavior of asphalt concrete used as impervious core in embankment dams. J. Geotech. Geoenviron. Eng. (ASCE) 137 (5), 536–544.

Wang, W., Höeg, K., 2016. Simplified material model for analysis of asphalt core in embankment dams. Constr. Build. Mater. 124 (2016), 199–207.

Wang, W., Zhang, Y., Xu, T., 2017b. Design and construction of the Quxue asphalt core rockfill dam. Hydropower and Dams 24 (4), 87–92.

Zhang, Y., Höeg, K., Wang, W., Zhu, Y., 2013. Watertightness, cracking resistance, and self-healing of asphalt concrete used as a water barrier in dams. Can. Geotech. J. 50 (3), 275–287.

Zhang, Y., Wang, W., Zhu, Y., 2015. Investigation on conditions of hydraulic fracturing for asphalt concrete used as impervious core in dams. Constr. Build. Mater. 93 (2015), 775–781.